Macroeconomic Dynamics, **25**, 2021, 1538–1568. Printed in the United States of America.
doi:10.1017/S1365100519000774

HETEROGENEOUS EXPECTATIONS AND ASSET PRICE DYNAMICS

Noemi Schmitt
University of Bamberg

Within the seminal asset-pricing model by Brock and Hommes (*Journal of Economic Dynamics Control* 22, 1235–1274, 1998), heterogeneous boundedly rational agents choose between a fixed number of expectation rules to forecast asset prices. However, agents' heterogeneity is limited in the sense that they typically switch between a representative technical and a representative fundamental expectation rule. Here, we generalize their framework by considering that all agents follow their own time-varying technical and fundamental expectation rules. Estimating our model using the method of simulated moments reveals that it is able to explain the statistical properties of the daily and monthly behavior of the S&P500 quite well. Moreover, our analysis reveals that heterogeneity is not only a realistic model property but clearly helps to explain the intricate dynamics of financial markets.

Keywords: Financial Markets, Stylized Facts, Agent-Based Models, Heterogeneity and Coordination

1. INTRODUCTION

One of the most influential asset-pricing models with heterogeneous beliefs is the one by Brock and Hommes (1998). In their setup, agents choose from a finite set of different expectation rules to forecast prices and update their choices according to past realized profits. Moreover, agents are boundedly rational in the sense that they tend to switch toward forecasting strategies that have performed better in the past. A main result offered by their model is that complicated asset price dynamics may arise when the intensity of choice to switch predictors is high. The evolutionary predictor selection approach has also been used by Brock and Hommes (1997), who call the bifurcation route to increasingly complex dynamics as the intensity of choice to switch forecasting strategies increases a *rational route to randomness*.

Presented at the 25th International Conference on Computing in Economics and Finance (CEF), June 28–June 30, 2019, Ottawa, Canada, and at the 23rd Annual Workshop on Economic Science with Heterogeneous Interacting Agents (WEHIA), June 28–July 2, 2018, Tokyo, Japan. We thank Frank Westerhoff, Christian Proaño, Roberto Dieci, and Remco Zwinkels for their valuable feedback. The paper also benefited from constructive comments of two anonymous referees and an associate editor. Address correspondence to: Noemi Schmitt, Department of Economics, University of Bamberg, Feldkirchenstrasse 21, 96045 Bamberg, Germany. e-mail: noemi.schmitt@uni-bamberg.de. Phone: +49 951 8632748.

© 2020 Cambridge University Press 1469-8056/20

https://doi.org/10.1017/S1365100519000774 Published online by Cambridge University Press

Due to their power and great economic appeal, the models by Brock and Hommes (1997, 1998) have been extended in various interesting directions. For instance, Brock et al. (2009) introduce Arrow securities and demonstrate that adding more hedging instruments may destabilize market dynamics. Similarly, Anufriev and Tuinstra (2013) introduce short-selling constraints to analyze whether such a policy measure can stabilize financial markets. In De Grauwe and Grimaldi (2006), the switching mechanism is implemented in a nonlinear exchange rate model and it is shown that important features of exchange rates can be reproduced. Of course, many more extensions exist in the literature. See Hommes (2013) for an excellent review. Note also that Boswijk et al. (2007), using yearly S&P500 data, and Hommes and 't Veld (2017), using quarterly S&P500 data, provide strong empirical support for the approach by Brock and Hommes (1998).

In the most elementary version of their model, all agents switch between a representative technical and a representative fundamental expectation rule. In reality, however, agents' expectations differ. Empirical studies, such as the ones by Ito (1990), MacDonald and Marsh (1996), Menkhoff et al. (2009), or Ter Ellen et al. (2013), explicitly stress that expectations of professional forecasters are heterogeneous. Anufriev and Hommes (2012), reinvestigating the laboratory experiments of Hommes et al. (2005, 2008), also find that heterogeneous expectations are crucial to describe the boom-and-bust dynamics of financial markets. However, forecasters' behavior is not independent. A striking and robust finding of the learning to forecast experiment by Hommes et al. (2005) is that individuals tend to coordinate on using the same type of simple prediction strategies. Furthermore, speculators are subject to herding behavior, which has already been documented in several empirical studies. Trueman (1994), for instance, analyzes forecasts by financial analysts and reports that they tend to release forecasts similar to those released by others. Welch (2000) also detects a positive influence of security analysts' buy or sell recommendations on those of others. Note that a number of agent-based financial market address speculators' herding behavior, see, for instance, Kirman (1993), Lux (1995) or Cont and Bouchaud (2000).

Against this background, we want to generalize the framework by Brock and Hommes (1998) by considering that all agents follow their own time-varying technical and fundamental expectation rules, that is, we assume that all agents have different expectations. Since speculators do not trade independently from each other, we also assume that our agents' forecasts are correlated. Thus, the first goal of this contribution is to provide an agent-based setup of the model by Brock and Hommes (1998). Moreover, we want to explore the extent to which the generalized model can explain the stylized facts of financial markets. For this purpose, we estimate our model using the method of simulated moments and find that our approach matches the daily and monthly behavior of the S&P500 quite well. In this sense, our paper complements the studies by Boswijk et al. (2007) and Hommes and 't Veld (2017), who rely on yearly and quarterly S&P500

https://doi.org/10.1017/S1365100519000774 Published online by Cambridge University Press

data, respectively. Finally, our analysis reveals a novel explanation for the intricate behavior of financial markets. As we will see, the simplicity of our approach allows analytical insights that prove to be helpful in understanding how the model functions.

Note that the model by Brock and Hommes (1998) was motivated by the Santa Fe artificial stock market model by LeBaron et al. (1999). They construct a framework in which a large number of interacting agents relies on an individual set of many different forecasting rules. Agents learn and modify their sets of forecasting rules by eliminating poorly performing rules and developing new ones. As it turns out, their large-scale setup is able to replicate certain stylized facts of financial markets. Since such a framework is not analytically tractable, Brock and Hommes (1998) provide and analyze a simple version of such an adaptive belief system. By adding individual heterogeneity to their approach, our paper aims at bridging the gap between large-scale and small-scale models to improve our understanding of financial markets. Related to our approach is the work by Brock et al. (2005) who generalize the model by Brock and Hommes (1998) to an evolutionary system with many different trader types and show that its dynamical behavior can be approximated by the notion of a large type limit (LTL). They demonstrate that all generic and persistent features of an adaptive belief system with many trader types, such as steady state, local bifurcations, or (quasi-)periodic dynamics, also occur in the LTL.[1] In principle, the LTL theory also forms a bridge between analytical tractable models and the agent-based approach. However, the focus of our paper is different since we aim at explaining the stylized facts of stock markets. For general surveys on agent-based financial market models, see, for example, LeBaron (2006), Chiarella et al. (2009), or Lux (2009).

The remainder of this paper is organized as follows. In Section 2, we extend the seminal model by Brock and Hommes (1998) by assuming that all agents have heterogeneous expectations. After presenting the setup of our model, we analyze its deterministic skeleton in Section 3. In particular, we derive the dynamical system of our deterministic model and analyze its steady states and their local asymptotic stability. In Section 4, we estimate our model and demonstrate that the stochastic version of our model replicates a number of important stylized facts of financial markets. Section 5 concludes our paper and highlights a few avenues for future research.

2. MODEL SETUP

In this section, we consider the asset-pricing model with heterogeneous boundedly rational agents by Brock and Hommes (1998) and provide an agent-based setup of their model. They assume that agents know the risky asset's fundamental value but choose from a finite set of different beliefs to forecast its price. In their elementary setup, these rules comprise a single fundamental and a single technical prediction rule. Agents' choices are updated in each period and depend on

https://doi.org/10.1017/S1365100519000774 Published online by Cambridge University Press

the past performance of the forecasting rules. In contrast to Brock and Hommes (1998), we assume that each agent follows his own fundamental and technical prediction rule, that is, all agents have different expectations. However, agents' forecasts are correlated to some extent.

Let us turn to the details of the model. Agents can invest in a risk-free asset or in a risky asset. The risk-free asset is in perfectly elastic supply and pays a fixed rate of return r, while the risky asset is in zero net supply and pays an uncertain dividend y_t. By defining p_t as the price per share (ex-dividend) of the risky asset at time t, the wealth of agent i in period $t+1$ can be expressed as

$$W^i_{t+1} = (1+r)W^i_t + (p_{t+1} + y_{t+1} - (1+r)p_t)z^i_t, \tag{1}$$

where z^i_t represents the demand of agent i for the risky asset at time t. Since agents are assumed to behave as myopic mean-variance maximizers, their demand for the risky asset follows from

$$\max_{z^i_t} \left\{ E^i_t[W^i_{t+1}] - \frac{a}{2} V^i_t[W^i_{t+1}] \right\}, \tag{2}$$

where $E^i_t[W^i_{t+1}]$ and $V^i_t[W^i_{t+1}]$ denote agent i's beliefs about the conditional expectation and conditional variance of his wealth in period $t+1$ and parameter a represents a uniform risk aversion coefficient. Moreover, it is assumed that beliefs about conditional variance are constant and uniform across all agents, that is, $V^i_t[p_{t+1} + y_{t+1} - (1+r)p_t] = \sigma^2$ for all t and agents i.[2] Solving (2) for z^i_t then yields

$$z^i_t = \frac{E^i_t[p_{t+1} + y_{t+1} - (1+r)p_t]}{aV^i_t[p_{t+1} + y_{t+1} - (1+r)p_t]} = \frac{E^i_t[p_{t+1} + y_{t+1} - (1+r)p_t]}{a\sigma^2}. \tag{3}$$

As in Brock and Hommes (1998), the supply of shares per agent is denoted by z^s and is assumed to be fixed. Equilibrium of demand and supply can therefore be formalized as

$$\sum_{i=1}^{N} \frac{E^i_t[p_{t+1} + y_{t+1} - (1+r)p_t]}{a\sigma^2} = Nz^s, \tag{4}$$

where N denotes the total number of agents. By assuming a zero supply of outside shares, that is, $z^s = 0$,[3] the market equilibrium equation becomes

$$(1+r)p_t = \frac{\sum_{i=1}^{N} E^i_t[p_{t+1} + y_{t+1}]}{N}. \tag{5}$$

Before agents' expectations about future prices and dividends are specified, let us recall how the fundamental price is derived. When all agents have homogeneous expectations, equation (5) simplifies to

$$(1+r)p_t = E_t[p_{t+1} + y_{t+1}], \tag{6}$$

https://doi.org/10.1017/S1365100519000774 Published online by Cambridge University Press

which can be used repeatedly. If a perfectly rational world is then assumed and the transversality condition

$$\lim_{t\to\infty} \frac{E_t[p_{t+k}]}{(1+r)^k} = 0 \tag{7}$$

holds, the fundamental price can be determined by the discounted sum of expected future dividends, that is,

$$p_t^* = \sum_{k=1}^{\infty} \frac{E_t[y_{t+k}]}{(1+r)^k}. \tag{8}$$

Since Brock and Hommes (1998) consider an IID dividend process y_t with mean $E[y_t] = \bar{y}$, the fundamental price is constant and given by

$$p^* = \sum_{k=1}^{\infty} \frac{\bar{y}}{(1+r)^k} = \frac{\bar{y}}{r}. \tag{9}$$

Beliefs about future dividends are assumed to be identical across all agents and correspond to the conditional expectation, that is,

$$E_t^i[y_{t+1}] = E_t[y_{t+1}] = \bar{y}, \tag{10}$$

which also implies that all agents know the fundamental value p^* that would prevail in a perfectly rational world. However, the equilibrium price can then be expressed as

$$p_t = \frac{1}{1+r}\left(\bar{y} + \frac{\sum_{i=1}^{N} E_t^i[p_{t+1}]}{N}\right). \tag{11}$$

Brock and Hommes (1998) assume that expectations about future prices are heterogeneous and consider various types of belief. In this paper, we assume that agents choose among two general types of forecasting rules, that is, agents can rely either on technical or on fundamental analysis to predict prices.[4] This can be formalized by

$$E_t^i[p_{t+1}] = \begin{cases} E_t^{C,i}[p_{t+1}] & \text{if } I_t^i = 1 \\ E_t^{F,i}[p_{t+1}] & \text{if } I_t^i = 0 \end{cases}, \tag{12}$$

where $E_t^{C,i}[p_{t+1}]$ and $E_t^{F,i}[p_{t+1}]$ represent agent i's price forecasts using technical and fundamental analysis, respectively. Accordingly, agent i chooses the technical (fundamental) prediction rule when the indicator function I_t^i, defined in (19), takes the value 1 (0).

Technical analysis seeks to extrapolate past price trends into the future (Murphy (1999)), while fundamentalists believe that asset prices revert toward their fundamental value (Graham and Dodd (1951)). Since there is a wide variety of technical and fundamental forecasting rules, we follow Westerhoff and Dieci (2006) and

https://doi.org/10.1017/S1365100519000774 Published online by Cambridge University Press

Franke (2010) and capture at least part of the rules' heterogeneity by adding random terms to the basic principles. In contrast to their model setups, however, the noise affects agents on an individual level, which implies that all agents have different expectations. Accordingly, agent i's technical and fundamental price forecasts consist of two components and are specified by

$$E_t^{C,i}[p_{t+1}] = p_{t-1} + (1-g)(p^* - p_{t-1}) + p_{t-1}\sigma^C \epsilon_t^{C,i} \tag{13}$$

and

$$E_t^{F,i}[p_{t+1}] = p_{t-1} + (1-v)(p^* - p_{t-1}) + p_{t-1}\sigma^F \epsilon_t^{F,i}, \tag{14}$$

where $g > 1$ and $0 < v < 1$. Note that $\epsilon_t^{C,i}$ and $\epsilon_t^{F,i}$ represent random terms while σ^C and σ^F denote the corresponding standard deviations.[5] The first parts of (13) and (14) represent the core principles of the forecasting rules, where g and v denote the coefficients of the two types of belief. As can be seen, both forecasting rules predict the next period's price by extrapolating past deviations from the fundamental value. If agents follow the technical price forecast $E_t^{C,i}$, they expect the deviation of the stock price to increase. Note that this type of agents is also referred to as chartists. The higher parameter g, the stronger agents extrapolate the latest observed price deviation. Such a specification of the technical prediction rule is also used, among others, by Day and Huang (1990), Boswijk et al. (2007), Hommes and 't Veld (2017), and Westerhoff and Franke (2012). If agents choose to be fundamentalists, they believe that the next period's price will move toward the fundamental value by a factor v. Since $0 < v < 1$, the expected mean reversion is higher when the v is closer to 0.

The second parts of belief types (13) and (14) are the stochastic components, reflecting random digressions from the rules' deterministic cores. Although all agents follow their own individual technical and fundamental forecasting rules, their behavior is not independent. Supported by the empirical and experimental studies reported in the introduction, we assume that agents coordinate and that they are subject to herding behavior. We therefore follow Schmitt and Westerhoff (2017) and assume that $\epsilon_t^C = \{\epsilon_t^{C,1}, \epsilon_t^{C,2}, ..., \epsilon_t^{C,N}\}'$ and $\epsilon_t^F = \{\epsilon_t^{F,1}, \epsilon_t^{F,2}, ..., \epsilon_t^{F,N}\}'$ are multivariate standard normally distributed random variables, that is, $\epsilon_t^C \sim \mathcal{N}(\mu^C, \Sigma^C)$ and $\epsilon_t^F \sim \mathcal{N}(\mu^F, \Sigma^F)$. Of course, μ^C and μ^F are zero vectors. The variance–covariance matrices are given by

$$\Sigma^j = \begin{Bmatrix} 1 & \rho^j & \dots & \rho^j \\ \rho^j & 1 & & \vdots \\ \vdots & & \ddots & \rho^j \\ \rho^j & \dots & \rho^j & 1 \end{Bmatrix}, \quad j = C, F, \tag{15}$$

where ρ^C and ρ^F denote the correlation coefficients of technical and fundamental random signals, respectively. For instance, if $\rho^C = \rho^F = 0$, agents' random signals are not correlated, implying that their forecasts display maximal heterogeneity.

https://doi.org/10.1017/S1365100519000774 Published online by Cambridge University Press

Alternatively, if $\rho^C = \rho^F = 1$, agents' random signals are perfectly correlated. In this case, agents either follow a representative stochastic technical prediction rule or a representative stochastic fundamental trading rule, as is the case in Westerhoff and Dieci (2006) and Franke (2010). As we will see in Section 4, the empirical analysis of our model reveals that $0 < \rho^C, \rho^F < 1$, that is, agents' forecasting rules are partially correlated.[6]

Agents switch between technical and fundamental analysis with respect to a certain fitness measure. To be more precise, the probabilities that agents will choose one of the two predictors are updated according to their past performance. The more successful the forecasting rule, the more probable it is that agents will follow it. These probabilities are determined using the multinomial discrete choice model by Manski and McFadden (1981). The probabilities that agent i will choose technical and fundamental analysis are therefore given by

$$\pi_t^{j,i} = \frac{\exp\left[\beta U_{t-1}^{j,i}\right]}{\exp\left[\beta U_{t-1}^{C,i}\right] + \exp\left[\beta U_{t-1}^{F,i}\right]}, \quad j = C, F, \tag{16}$$

where $U_{t-1}^{C,i}$ and $U_{t-1}^{F,i}$ measure the fitness of the two forecasts in period $t-1$. Parameter β is the intensity of choice and measures how quickly agents switch to the more successful forecast. The higher the intensity of choice, the greater the probability that agent i will opt for the strategy with the higher fitness. For $\beta = 0$, the probability that agent i will use technical or fundamental analysis is 50%. For $\beta = \infty$, agent i will select with a probability of 100% the forecasting rule that had a higher fitness in the previous period. Note that $\exp[\beta U_{t-1}^{C,i}] + \exp[\beta U_{t-1}^{F,i}]$ is used as a normalization factor to make sure that probabilities add up to 1. Hence, the probability that agent i will opt for the fundamental (technical) forecast can also be expressed as $\pi_t^{F,i} = 1 - \pi_t^{C,i}$ ($\pi_t^{C,i} = 1 - \pi_t^{F,i}$).

Fitness is determined by accumulated past profits.[7] Since the realized excess return of the risky asset over the risk-free asset can be computed as $R_t = p_t + y_t - (1+r)p_{t-1}$[8], the performance of the two predictors can be defined by

$$U_t^{j,i} = (1-\mu)(p_t + y_t - (1+r)p_{t-1})z_{t-1}^{j,i} + \mu U_{t-1}^{j,i}, \quad j = C, F, \tag{17}$$

where

$$z_{t-1}^{j,i} = \frac{E_{t-1}^{j,i}[p_t] + \bar{y} - (1+r)p_{t-1}}{a\sigma^2}, \quad j = C, F \tag{18}$$

express agent i's technical and fundamental demand for the risky asset in the previous period, respectively, and $0 \leq \mu < 1$ is a memory that measures how strongly fitness measures depend on current and past profits. For $\mu = 0$, agents have no memory and the performance of the two types of belief is given by the most recent profit that would have been realized by agent i if he had chosen technical or fundamental analysis. If μ increases, these fitness measures depend more strongly on the accumulated profits that he would have realized in the past.[9]

https://doi.org/10.1017/S1365100519000774 Published online by Cambridge University Press

A comment is in order at this point. For analytical tractability, Brock and Hommes (1998) assume that all agents switch between a representative technical and a representative fundamental expectation rule. As a result, all agents obtain identical trading profits for their two expectation rules, implying that the fitness measures as well as the discrete choice probabilities are equal across agents of the same type. In reality, however, agents' expectations differ. Agents' demand functions, their profit opportunity, the rules' past performance, and the discrete choice probabilities therefore also have an explicit agent-specific nature in real financial markets. It is precisely this observation that forms the core of our model.

Recall from (12) that agent i chooses the technical (fundamental) forecast if the indicator function takes the value 1 (0), that is, $I_t^i = 1$ ($I_t^i = 0$). Since the probability that agent i will opt for technical (fundamental) analysis is represented by $\pi_t^{C,i}$ ($\pi_t^{F,i}$), the indicator function can be formalized by

$$I_t^i = \begin{cases} 1 & \text{with prob } \pi_t^{C,i} \\ 0 & \text{with prob } \pi_t^{F,i} \end{cases}, \tag{19}$$

which is introduced to keep track of the number of agents that follow technical and fundamental forecasting rules. These can now easily be defined by

$$N_t^C = \sum_{i=1}^{N} I_t^i \tag{20}$$

and

$$N_t^F = \sum_{i=1}^{N} \left(1 - I_t^i\right) \tag{21}$$

respectively. Due to $N_t^C + N_t^F = N$, the relative numbers of chartists and fundamentalists are given by

$$W_t^j = \frac{N_t^j}{N}, \quad j = C, F. \tag{22}$$

Of course, their weights add up to 1, which is why the relative number of fundamentalists (chartists) can also be formalized by $W_t^F = 1 - W_t^C$ ($W_t^C = 1 - W_t^F$).

3. ANALYSIS OF THE MODEL'S DETERMINISTIC SKELETON

In this section, we study the underlying deterministic framework of our model. The analytical insights we gain will prove useful when discussing how our stochastic model functions in Section 4.[10] In Section 3.1, we derive the dynamical system of our deterministic model and analyze its steady states and their local asymptotic stability in Section 3.2. In Section 3.3, we introduce a parameter setting to illustrate the global behavior of our deterministic model.

https://doi.org/10.1017/S1365100519000774 Published online by Cambridge University Press

3.1. Dynamical System

To derive the dynamical system of our deterministic model, we set $\sigma^C = \sigma^F = 0$, assume $N \to \infty$, and rewrite the model in deviations from the fundamental value. In the process, we follow Brock and Hommes (1997, 1998) and introduce $x_t = p_t - p^*$. Forecasts about future prices then become

$$E_t^C[x_{t+1}] = g x_{t-1} \tag{23}$$

and

$$E_t^F[x_{t+1}] = v x_{t-1}. \tag{24}$$

Moreover, we use the fact that the fundamental price satisfies $(1+r)p_t^* = E_t[p_{t+1}^* + y_{t+1}]$ and express the equilibrium equation as

$$x_t = \frac{1}{(1+r)}(W_{t-1}^C E_t^C[x_{t+1}] + W_{t-1}^F E_t^F[x_{t+1}]), \tag{25}$$

where

$$W_t^C = \frac{\exp\left[\beta U_t^C\right]}{\exp\left[\beta U_t^C\right] + \exp\left[\beta U_t^F\right]} \tag{26}$$

and

$$W_t^F = 1 - W_t^C. \tag{27}$$

Note that setting random terms equal to zero implies that forecasting rules only consist of the deterministic parts of the two types of belief which are equal across agents. Thus, agents either follow a representative technical or a representative fundamental prediction rule. Since profits of agents of the same type are then identical, the two fitness measures are equal across agents. These can also be rewritten in deviations from the fundamental value as

$$U_t^j = (1-\mu)(x_t - (1+r)x_{t-1})\frac{E_{t-1}^j[x_t] - (1+r)x_{t-1}}{a\sigma^2} + \mu U_{t-1}^j, \quad j = C, F. \tag{28}$$

Of course, equal fitness measures imply equal discrete choice probabilities, which is why the relative number of chartists and fundamentalists can also be defined by (26) and (27), respectively.[11]

Finally, we introduce the difference in fractions $m_t = W_t^F - W_t^C = \tanh[\frac{\beta}{2}(U_t^F - U_t^C)]$ and summarize the model's deterministic skeleton by the three-dimensional nonlinear system

$$S: \begin{cases} x_t = \frac{1}{(1+r)}\left(\frac{1-m_{t-1}}{2} g x_{t-1} + \frac{m_{t-1}+1}{2} v x_{t-1}\right) \\ q_t = x_{t-1} \\ m_t = \tanh\left[\frac{\beta}{2}\left\{(1-\mu)(x_t - (1+r)x_{t-1})\frac{v q_{t-1} - g q_{t-1}}{a\sigma^2} + \mu \frac{2\,\mathrm{arctanh}[m_{t-1}]}{\beta}\right\}\right] \end{cases}, \tag{29}$$

where $q_t = x_{t-1}$ is an auxiliary variable.[12]

https://doi.org/10.1017/S1365100519000774 Published online by Cambridge University Press

3.2. Steady States and Local Asymptotic Stability

We are now ready to explore the existence and stability of steady states of (29). Our first set of results is summarized by:

PROPOSITION 1. *Assume* $r > 0$, $g > 1$, $0 < v < 1$ *and* $0 \leq \mu < 1$. *Let* $m^* = \frac{g+v-2(r+1)}{g-v}$, $x^*_{2/3} = \pm\sqrt{\frac{2a\sigma^2 \operatorname{arctanh}[\frac{g+v-2(r+1)}{g-v}]}{\beta r(g-v)}}$ *and* $q^*_{2/3} = x^*_{2/3}$. *Then:*

(i) For $g < 2(r+1) - v$, $S_1 = (0,0,0)$ *is the unique, locally stable (fundamental) steady state.*

(ii) At $g = 2(r+1) - v$, *a pitchfork bifurcation occurs, that is, two additional (non-fundamental) steady states are created.*

(iii) For $g > 2(r+1) - v$, *there exist three steady states* $S_1 = (0,0,0)$, $S_2 = (x^*_2, q^*_2, m^*)$ *and* $S_3 = (x^*_3, q^*_3, m^*)$; *the (fundamental) steady state* S_1 *is unstable.*

Proof. It follows from the pricing equation that a steady state must satisfy

$$(1+r)x^* = \frac{1-m^*}{2} g x^* + \frac{m^*+1}{2} v x^*,$$

which implies that $x^* = 0$ or $m^* = \frac{g+v-2(r+1)}{g-v}$. For $x^* = 0$, we have $q^* = 0$ and obtain $\operatorname{arctanh}[m^*](1-\mu) = 0$ from the equation of the difference in fractions. Since $\mu \neq 1$, it follows that the steady-state difference in fractions is $m^* = 0$. Moreover,

$$m^* = \tanh\left[\frac{\beta}{2}\left\{(1-\mu)(x^* - (1+r)x^*)\frac{vx^* - gx^*}{a\sigma^2} + \mu\frac{2\operatorname{arctanh}[m^*]}{\beta}\right\}\right], \quad \textbf{(30)}$$

where $m^* = \frac{g+v-2(r+1)}{g-v}$, yields

$$x^{*^2} = \frac{2a\sigma^2 \operatorname{arctanh}\left[\frac{g+v-2(r+1)}{g-v}\right]}{\beta r(g-v)}.$$

Note that $-1 < m^* < 0$ for $(r+1) < g < 2(r+1) - v$, while we have $0 < m^* < 1$ for $g > 2(r+1) - v$. However, equation (30) only has two solutions $\pm x^*$ if $g > 2(r+1) - v$. Thus, the fundamental steady state is given by $S_1 = (0,0,0)$ and there exist two non-fundamental steady states $S_2 = (x^*, q^*, m^*)$ and $S_3 = (-x^*, -q^*, m^*)$, where $m^* = \frac{g+v-2(r+1)}{g-v}$ and x^* is the positive solution of (30) if and only if $g > 2(r+1) - v$.

From the Jacobian of the fundamental steady state S_1, that is,

$$J(S_1) = \begin{pmatrix} \frac{g+v}{2(1+r)} & 0 & 0 \\ 1 & 0 & 0 \\ 0 & 0 & \mu \end{pmatrix},$$

we obtain $\lambda_1 = \frac{g+v}{2(1+r)}$, $\lambda_2 = 0$, and $\lambda_3 = \mu$. Since $0 \leq \mu < 1$, the eigenvalues λ_2 and λ_3 always lie inside the unit circle. The eigenvalue λ_1 is larger than $+1$ for

https://doi.org/10.1017/S1365100519000774 Published online by Cambridge University Press

$g > 2(r+1) - v$, the case for which two additional steady states exist. Thus, we have a pitchfork bifurcation at $g = 2(r+1) - v$ and the first eigenvalue lies in the interval $(0, 1)$ if and only if $g < 2(r+1) - v$. ■

As stated above, if $g < 2(r+1) - v$, the deterministic skeleton of our model has a unique, locally stable steady state where the price equals its fundamental value. We therefore call this the fundamental steady state. Since we have $p_t = p^*$ or $x^* = 0$ at S_1, both predictors yield the same forecast and the difference in profits is zero. Hence, half of the agents use the technical forecasting rule and the other half use the fundamental forecasting rule, that is, $W_t^C = W_t^F = 0.5$ or $m^* = 0$. However, when chartists extrapolate more strongly, that is, when parameter g increases to $g = 2(r+1) - v$, a pitchfork bifurcation occurs. The fundamental steady state S_1 then becomes unstable and two additional non-fundamental steady states S_2 and S_3 are created. The next result is:

PROPOSITION 2. *Suppose there exist the non-fundamental steady states* $S_2 = (x_2^*, q_2^*, m^*)$ *and* $S_3 = (x_3^*, q_3^*, m^*)$ *as in Proposition 1, that is,* $g > 2(r+1) - v$. *For values of g that are slightly larger than* $2(r+1) - v$, S_2 *and* S_3 *are locally stable. However, if g is further increased, the non-fundamental steady states undergo a Neimark–Sacker bifurcation and become unstable.*

Proof. The characteristic polynomial of the Jacobian computed at the non-fundamental steady states S_2 and S_3 is given by

$$p(\lambda) = \lambda^3 + \lambda^2(Z - 1 - \mu) + \lambda(\mu - Z - rZ) - rZ, \tag{31}$$

where

$$Z = \frac{-2(g - r - 1)(1 + r - v)(1 - \mu)\,\operatorname{arctanh}\left[\frac{g+v-2(r+1)}{g-v}\right]}{r(1+r)(g-v)}.$$

At the pitchfork bifurcation value $g = 2(r+1) - v$, we have $m^* = 0$ and therefore $Z = 0$. The characteristic equation (31) then yields $\lambda_1 = 1$, $\lambda_2 = 0$ and $\lambda_3 = \mu$. When parameter g increases slightly, Z becomes negative and we obtain three real eigenvalues inside the unit circle. Thus, the two non-fundamental steady states are stable for g slightly larger than $2(r+1) - v$. For $g \to \infty$, however, we have $Z \to -\infty$, which implies that one of the eigenvalues must cross the unit circle for some critical value of g and $S_{2/3} = (x_{2/3}^*, q_{2/3}^*, m^*)$ become unstable. Since $p(1) = -2rZ > 0$ and $p(-1) = 2(Z - \mu - 1) < 0$, two eigenvalues must be complex (see Brock and Hommes (1998)). Thus, the non-fundamental steady states become unstable by a Neimark–Sacker bifurcation. ■

Hence, for $g > 2(r+1) - v$, there also exist two non-fundamental steady states $S_{2/3} = (x_{2/3}^*, q_{2/3}^*, m^*)$, where $x_{2/3}^* = \pm\sqrt{2a\sigma^2 \operatorname{arctanh}[\frac{g+v-2(r+1)}{g-v}]/\beta r(g-v)}$, $q_{2/3}^* = x_{2/3}^*$ and $m^* = \frac{g+v-2(r+1)}{g-v}$. While one of these non-fundamental steady states is above the fundamental steady state, the other is below it. Moreover,

https://doi.org/10.1017/S1365100519000774 Published online by Cambridge University Press

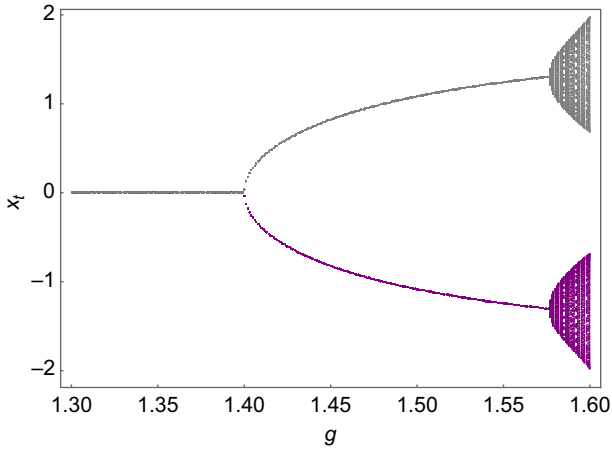


FIGURE 1. Bifurcation diagram for parameter g. Parameters are $r = 0.1$, $v = 0.8$, $\mu = 0.5$, $a\sigma^2 = 1$, $\beta = 3.5$, and $1.3 \leq g \leq 1.6$.

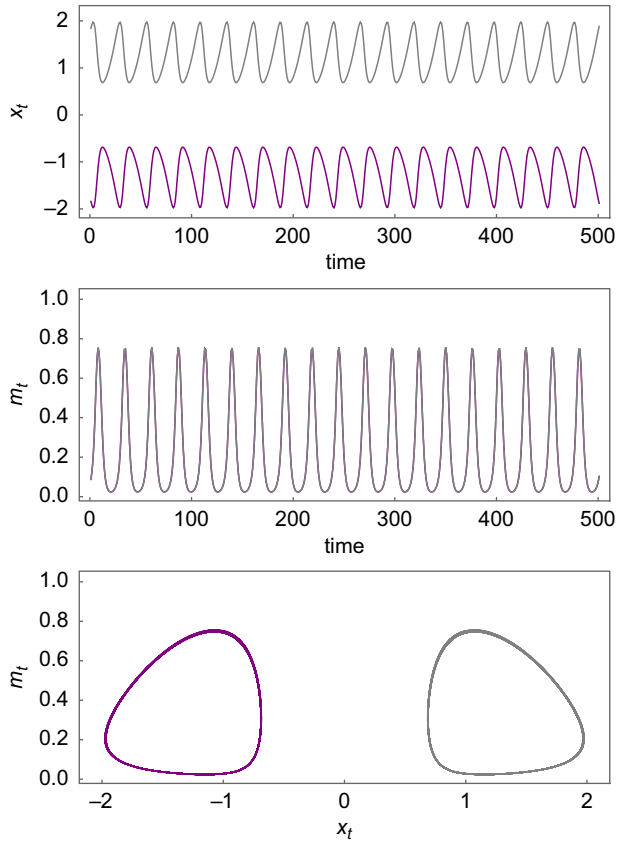
the deviations of x_2^* and x_3^* from the fundamental steady state increase with parameter g. This can be explained as follows. When chartists extrapolate the price deviation more strongly, prices diverge further from the fundamental value, that is, x_2^* (x_3^*) increases (decreases). Since fundamental analysis then becomes more attractive, more and more agents choose the fundamental predictor, implying that m^* increases. At some critical value for g, however, the two non-fundamental steady states become unstable by a Neimark–Sacker bifurcation, in which invariant circles around each of the two non-fundamental steady states arise.[13]

3.3. Numerical Illustration

To illustrate our analytical results, we set $r = 0.1$, $v = 0.8$, $\mu = 0.5$, $a\sigma^2 = 1$, and $\beta = 3.5$ and show in Figure 1 the dynamical behavior of our deterministic model for increasing values of g. As can be seen, the fundamental steady state is stable for $g < 2(r + 1) - v = 1.4$. At $g = 1.4$, $x^* = 0$ becomes unstable and two additional steady states emerge. For $1.4 < g < 1.58$, our dynamical system may converge to the positive or to the negative non-fundamental steady state. As g increases further, the two non-fundamental steady states also become destabilized and (quasi-)periodic dynamics arises, as illustrated in Figure 2.

Figure 2 shows the dynamics of our deterministic model for $g = 1.6$. While the first two panels show time series of price deviations and differences in fractions, the third panel illustrates the attractors in the phase space.[14] It can be seen from the top panel that prices either cycle around the positive or around the negative unstable non-fundamental steady state, given by $x_2^* = 1.35$ and $x_3^* = -1.35$. The second panel shows the corresponding time series of the difference in fractions.

https://doi.org/10.1017/S1365100519000774 Published online by Cambridge University Press



Note. The first two panels illustrate the evolution of price deviations and differences in fractions for 500 periods, while the third panel shows phase plots in the (x_t, m_t) plane. Parameters are $r = 0.1$, $v = 0.8$, $\mu = 0.5$, $a\sigma^2 = 1$, and $\beta = 3.5$.

FIGURE 2. Dynamics of our deterministic skeleton for $g = 1.6$.

Note that $m^* = 0.25$ and that only one line is visible as the two time series overlap. The attractors plotted in the third panel also reveal that there are coexisting invariant circles around each of the two unstable non-fundamental steady states. However, if g is increased further, the dynamics quickly explodes and prices diverge to infinity.

4. STOCHASTIC DYNAMICS

Since the aim of our model is to explain the stylized facts of stock markets, we begin this section by briefly reviewing some of those statistical properties. Furthermore, we introduce some summary statistics to measure the stylized facts

https://doi.org/10.1017/S1365100519000774 Published online by Cambridge University Press

we seek to match. In Section 4.2, we report our estimation results for daily data and discuss the performance of our model. In Section 4.3, we show a snapshot of our dynamics and explain how the model functions. To check the robustness of our results, we use a different time series and reestimate our model. The results are presented in Section 4.4.

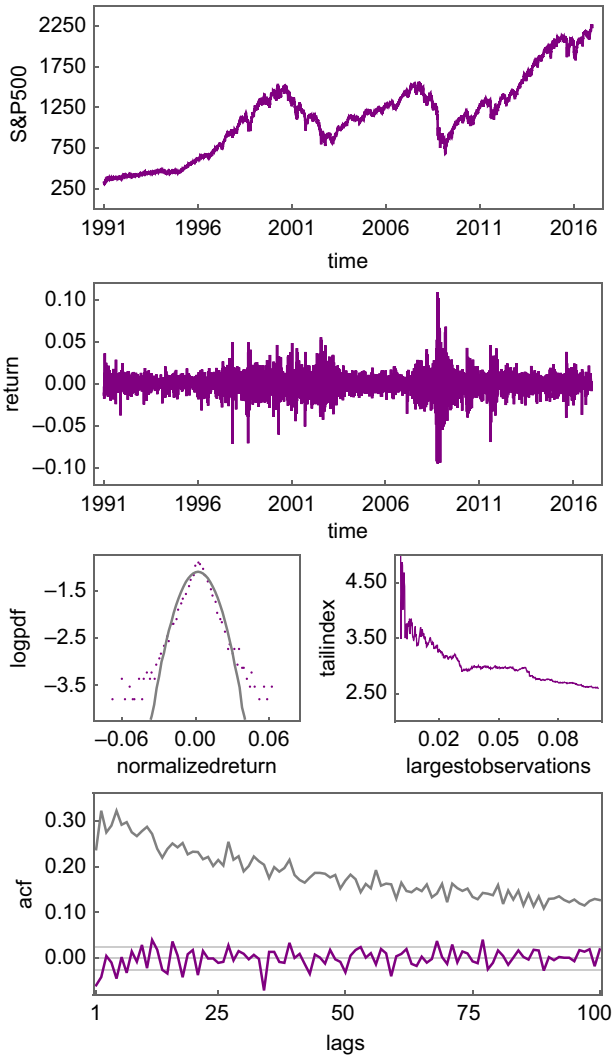
4.1. Stylized Facts of Stock Markets

As is well known, the dynamics of stock markets is characterized by (i) bubbles and crashes, (ii) excess volatility, (iii) fat-tailed return distributions, (iv) serially uncorrelated returns, and (v) volatility clustering. Statistical properties of financial markets are surveyed, for instance, by Mantegna and Stanley (2000), Cont (2001), Lux and Ausloos (2002), and Lux (2009). To illustrate these five universal features, we use a time series of the S&P500 stock market index that runs from January 1, 1991 to December 31, 2016 containing 6550 daily observations and show the dynamics in Figure 3. Moreover, we follow Franke and Westerhoff (2012) and quantify these features by a number of summary statistics, that is, "moments," which we present in Table 1.

In the top panel of Figure 3, we depict the daily evolution of the S&P500 between 1991 and 2016. As can be seen, stock prices show strong price appreciations as well as severe crashes. The corresponding return time series is plotted in the second panel. It reveals that stock prices fluctuate strongly and that extreme price changes of up to 11% exist. To measure overall volatility, we compute the standard deviation of returns and obtain a value of $V = 1.13\%$ per day. The left panel of the third row compares the log probability density functions of normalized returns (purple) and standard normally distributed returns (gray). The distribution of empirical returns obviously possesses a higher concentration around the mean, thinner shoulders, and again more probability mass in the tails than a normal distribution with identical mean and standard deviation. Since we also want to quantify the fat-tail property, we use the Hill tail index estimator (1975) and plot it as a function of the largest returns (in percent) on the right-hand side. Note that lower values for the tail index imply fatter tails. For instance, estimates on the largest 5% of the observations yield a tail index of $\alpha_{5.0} = 2.99$. However, when we compute the Hill tail index at the 5% level for normally distributed returns with $T = 6550$ and identical mean and standard deviation, we obtain a value of 6.49.

In the bottom panel of Figure 3, we show the autocorrelation functions of raw (purple) and absolute (gray) returns for the first 100 lags. The gray lines represent the 95% confidence bands. As the autocorrelation of raw returns is insignificant for almost all lags, it follows that the evolution of the S&P500 is close to a random walk. In contrast, absolute returns reveal autocorrelation coefficients that are highly significant for more than 100 lags, which implies a temporal persistence in volatility. It also becomes clear from the second panel of Figure 3 that periods of high volatility alternate with periods of low volatility. To quantify the absence

https://doi.org/10.1017/S1365100519000774 Published online by Cambridge University Press



Note. The panels show, from top to bottom, the evolution of the S&P500 between 1991 and 2016, the corresponding returns, the log probability density functions of normalized returns (purple) and standard normally distributed returns (gray), the Hill tail index estimator as a function of the largest returns and the autocorrelation functions of raw returns (purple) and absolute returns (gray), respectively.

FIGURE 3. The dynamics of the daily S&P500.

of autocorrelation in raw returns and the long memory in absolute returns, we choose to estimate the autocorrelation coefficients of raw returns for lags 1 and 2, and the autocorrelation coefficients of absolute returns for lags 3, 6, 12, 25, 50, and 100. These summary statistics are presented together with the two described above in the first lines of Table 1.

https://doi.org/10.1017/S1365100519000774 Published online by Cambridge University Press

TABLE 1. Moments of the daily S&P500

	V	$\alpha_{5.0}$	$ac\ r_1$	$ac\ r_2$	$ac\ \lvert r_3\rvert$
Measured	1.131	2.993	−0.059	−0.041	0.275
Lower bound	0.929	2.571	−0.105	−0.098	0.228
Upper bound	1.341	3.749	−0.017	0.011	0.325

	$ac\ \lvert r_6\rvert$	$ac\ \lvert r_{12}\rvert$	$ac\ \lvert r_{25}\rvert$	$ac\ \lvert r_{50}\rvert$	$ac\ \lvert r_{100}\rvert$
Measured	0.292	0.272	0.215	0.170	0.127
Lower bound	0.234	0.217	0.171	0.135	0.095
Upper bound	0.358	0.335	0.266	0.208	0.165

Note: The first lines contain estimates of the returns' standard deviation V, the Hill tail index $\alpha_{5.0}$, the autocorrelation coefficients of raw returns $ac\ r_i$ for lags 1 and 2, and the autocorrelation coefficients of absolute returns $ac\ |r_i|$ for lags $i \in \{3, 6, 12, 25, 50, 100\}$. The second and third lines show the lower and upper boundaries of the 95% confidence intervals around the summary statistics that are reported in the first lines. Estimates are based on a time series ranging from January 1, 1991 to December 31, 2016 that contains 6550 daily observations.

In the second and third lines of Table 1, we report for all 10 moments the lower and upper boundaries of the 95% confidence intervals of their bootstrapped frequency distributions. Due to the long-range dependence in the return time series, we follow Winker et al. (2007) and use a block bootstrap to compute the frequency distributions of the returns' standard deviation and the tail index. To this end, we subdivide the time series of the S&P500 into 26 blocks with 250 daily observations each, construct a new time series from 26 random draws (with replacement), and estimate the values of V and $\alpha_{5.0}$ from this new block bootstrapped time series. By repeating this 5000 times, we obtain the frequency distributions of the two statistics from which the lower and upper boundaries of the 95% confidence intervals can be computed. For the other distributions, however, we choose another bootstrap approach. Franke and Westerhoff (2016) highlight the fact that the long-range dependence in the return time series is always interrupted when two non-adjacent blocks are pasted; they suggest sampling single days together with the past data points required to compute lagged autocorrelations. Following their argument, we randomly draw 6550 observations with their consecutive data points from the S&P500 time series, compute the lagged autocorrelations, repeat this 5000 times, and obtain their distributions.

4.2. Estimation and Model Performance

Recall that the summary statistics (moments) were introduced to quantify the stylized facts we seek to match. Of course, the simulated moments should be as close as possible to the empirical moments. To this end, we employ the method of simulated moments to estimate our model. For pioneering contributions in this

https://doi.org/10.1017/S1365100519000774 Published online by Cambridge University Press

TABLE 2. Performance of the model

	V	$\alpha_{5.0}$	$ac\ r_1$	$ac\ r_2$	$ac\ \lvert r_3\rvert$
JMCR	0.904	0.794	0.966	0.974	0.936
0.324	$ac\ \lvert r_6\rvert$	$ac\ \lvert r_{12}\rvert$	$ac\ \lvert r_{25}\rvert$	$ac\ \lvert r_{50}\rvert$	$ac\ \lvert r_{100}\rvert$
	0.944	0.930	0.856	0.704	0.576

Note: The table shows the joint moment coverage ratio (JMCR) and the fractions of the individual moments' matching. Estimations are based on 500 simulation runs with 6550 observations each. Parameters are $r = 0.0002$, $F = 10$, $\bar{y} = 0.002$, $a\sigma^2 = 1$, $N = 300$, $g = 1.001$, $v = 0.989$, $\sigma^F = 0.004607$, $\sigma^C = 0.0265$, $\rho^C = \rho^F = 0.78$, $\beta = 1550$, and $\mu = 0.992$.

direction, see, for instance, Gilli and Winker (2003), Winker et al. (2007), or Franke (2009). As in Franke and Westerhoff (2012), we use the concept of a joint moment coverage ratio (JMCR) and aim to find the parameter setting that maximizes the fraction of simulation runs for which our simulated moments jointly fall into the 95% confidence intervals of their empirical counterparts. To be more precise, we count the number of simulation runs for which all 10 moments are contained in the empirical intervals and define the corresponding percentage as the JMCR. The estimation then searches for the parameter setting that maximizes the JMCR score.

However, not all of our model parameters are included in our estimation procedure. For instance, the value for the interest rate of the risk-free asset can be derived from empirical data. Since the current annual percentage rate is about 0.05, we obtain $r = 0.0002$ for the daily rate of return.[15] Moreover, the dynamics of our model does not depend on the level of the fundamental value, which is why we set $p^* = 10$, implying that $\bar{y} = 0.002$. To further reduce the number of parameters, we fix $N = 300$ and set $a\sigma^2 = 1$ as in Brock and Hommes (1998). We also make the simplifying assumption that the correlations of technical and fundamental random trading signals are equal, that is, $\rho^C = \rho^F$. Hence, there remain seven model parameters for which the maximization of the JMCR yields the following results:

$$g = 1.001,\ v = 0.989,\ \sigma^C = 0.0265,\ \sigma^F = 0.004607,$$
$$\rho^C = \rho^F = 0.78,\ \beta = 1550 \text{ and } \mu = 0.992.$$

The corresponding value of the JMCR is given by 0.324, that is, in 32.4% of the simulation runs all of our simulated moments drop in their empirical intervals. Given that our objective function is based on the joint matching of 10 different moments, such a ratio may be deemed as quite remarkable.[16]

In Table 2, we show how well our model matches the 10 individual moments. For instance, the volatility and the tail index fall in 90.4% and 79.4% of cases in the 95% confidence intervals of their empirical counterparts. The scores are even better for the autocorrelation coefficients of raw returns at lags 1 and 2.[17]

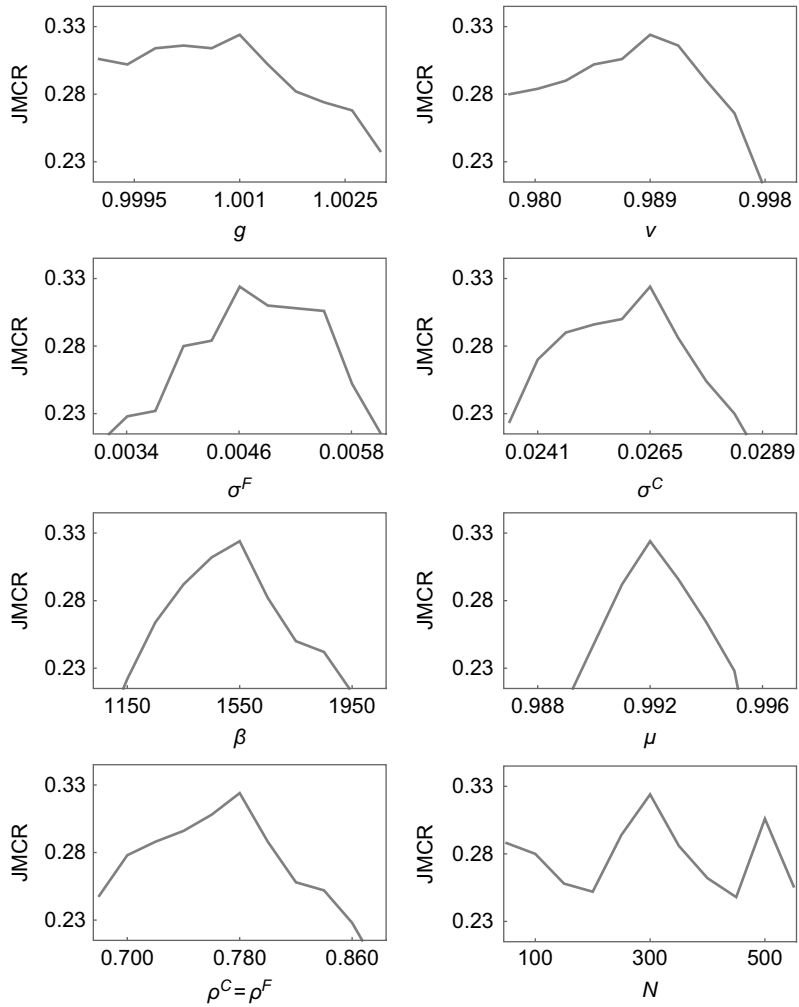
https://doi.org/10.1017/S1365100519000774 Published online by Cambridge University Press

These are given by 96.6% and 97.4%, respectively. As can be seen, the model's ability to generate persistence in volatility is also very good for lags 3, 6, 12, and 25. For higher lags, however, autocorrelations of absolute returns are slightly underestimated in some of the simulation runs, which is why we obtain lower scores for lags 50 and 100. Note that we also computed the average moment matching score for this parameter setting and obtained an astounding value of 85.8%, that is, on average, we match 85.8% of the empirical moments in a simulation run.

Note that our model parameters were identified by a multi-dimensional grid search in a predefined parameter space. Hence, we cannot rule out the existence of better performing parameter settings. However, any change in one of our estimated model parameters would result in a lower JMCR score, implying that we have found at least a local maximum of the JMCR. To visualize this, we show in Figure 4 how the model performance depends on our model parameters. For instance, the first panel reveals that the JMCR score decreases if we deviate from $g = 1.001$. Obviously, this is also true for $v = 0.989$, $\sigma^F = 0.004607$, $\sigma^C = 0.0265$, $\beta = 1550$, $\mu = 0.992$, and $\rho^C = \rho^F = 0.78$.[18] The last panel shows how the number of agents influences our model performance. Recall that parameter N was not included in our estimation procedure and that we optimized our parameter setting for $N = 300$. But, as one can see, our model also generates high JMCR scores for other values of N.

To illustrate the performance of our model, we depict a representative simulation run with 6550 observations in Figure 5. Since we want to compare our model dynamics directly with the dynamics of the S&P500, we use the same design as in Figure 3. Thus, the first panel shows the evolution of prices in the time domain. Apparently, the price of the risky asset fluctuates erratically around its fundamental value $p^* = 10$ and there are a number of periods in which prices either appreciate or depreciate strongly. Hence, our simulated price dynamics can also be characterized by bubbles and crashes. However, there is no long-run upward trend in prices since we assume that the fundamental value is constant. The second panel shows the corresponding return time series and reveals that price volatility is high. There are extreme price changes of up to 8.4% and the standard deviation of our simulated returns is given by 1.2%, that is, our model resembles the overall volatility of the S&P500 quite well. From the comparison of the log probability density functions of normalized (purple) and standard normally distributed (gray) returns, exhibited in the left panel of the third row, it becomes evident that our model also gives rise to fat tails. As can be seen, extreme returns occur more frequently than in the case of a normal distribution. This is also confirmed by estimates of the Hill tail index. In the right panel of the third row it can be observed, for instance, that we obtain a tail index of 3.51 at the 5% level. The bottom panel presents the autocorrelation functions of raw (purple) and absolute (gray) returns. As in the case of the S&P500, raw returns are basically serially uncorrelated while absolute returns display significant correlations for more than 100 lags.

https://doi.org/10.1017/S1365100519000774 Published online by Cambridge University Press



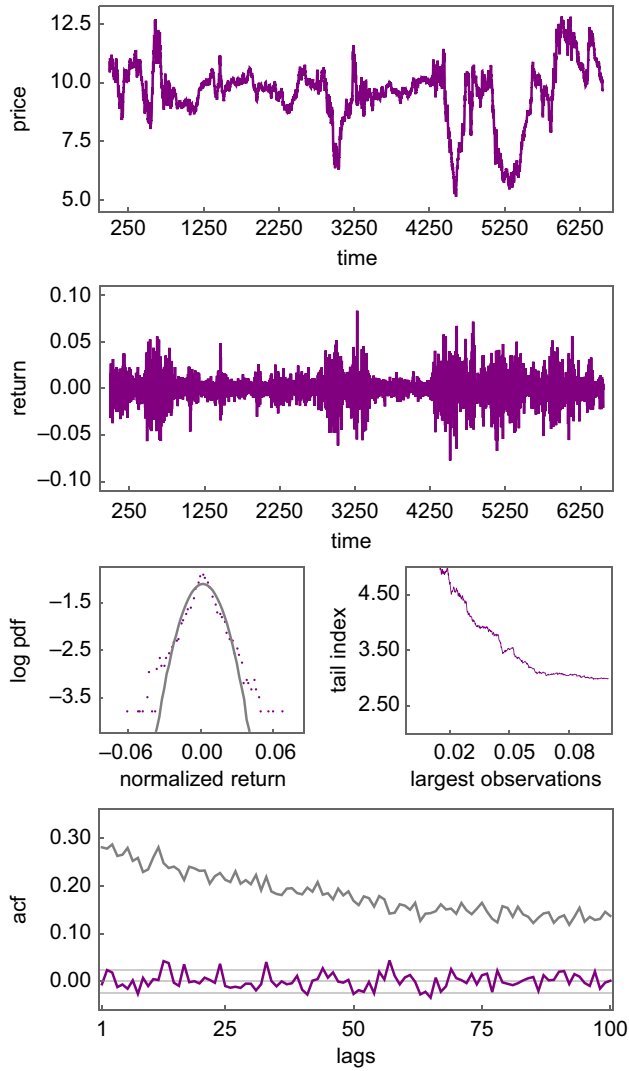
Note. The panels reveal how the JMCR score depends on parameters g, v, σ^F, σ^C, β, μ, $\rho^C = \rho^F$, and N. The computation of the JMCR is always based on 500 simulation runs.

FIGURE 4. Parameters' impact on the model's performance.

4.3. Functioning of the Model

Now that we have shown that our model is able to replicate the statistical properties of the daily behavior of the S&P500 quite well, we want to explain how it functions. For this purpose, we use the same simulation run as depicted in Figure 5 but focus only on the period between observations 2500 and 3700. The dynamics during this time is illustrated in Figure 6. The panels show, from top to bottom, the evolution of the price, the corresponding returns, and the weight of chartists, respectively. As can be seen, the weight of chartists is initially

https://doi.org/10.1017/S1365100519000774 Published online by Cambridge University Press

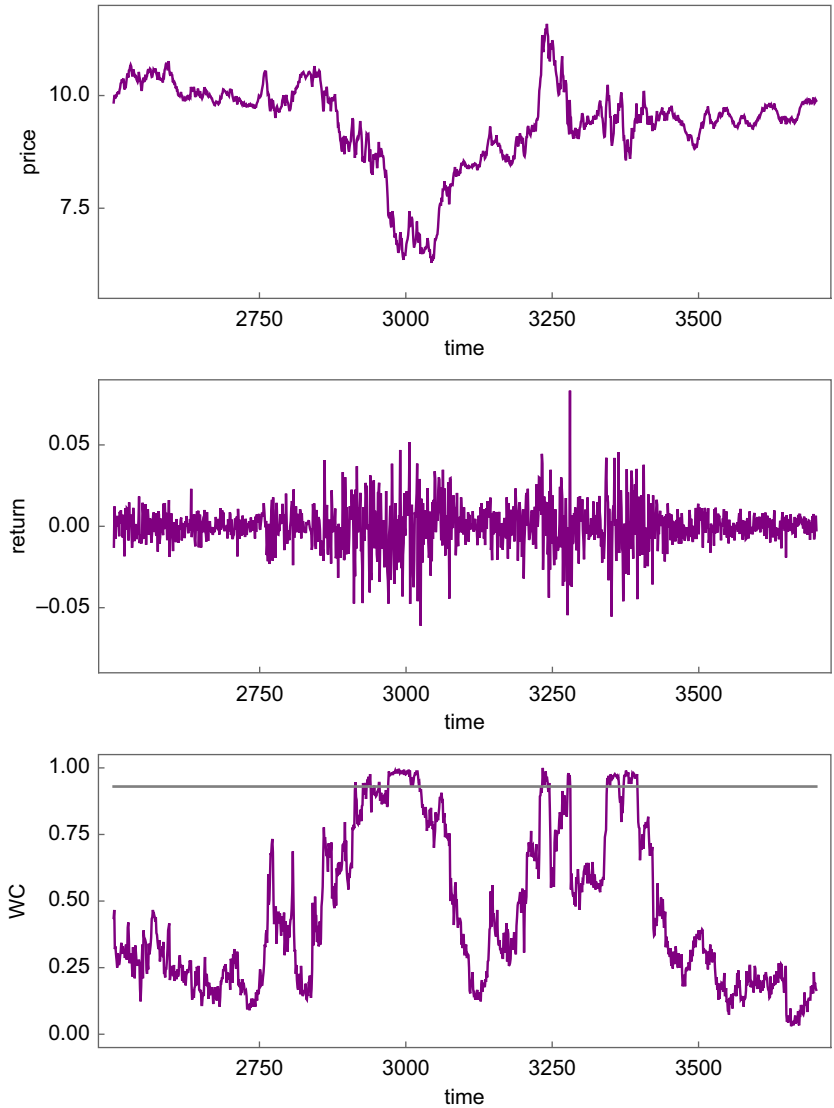


Note. The panels show, from top to bottom, the evolution of the price, the returns, the log probability density functions of normalized returns (purple) and standard normally distributed returns (gray), the Hill tail index estimator as a function of the largest returns and the autocorrelation functions of raw returns (purple) and absolute returns (gray), respectively. The simulation run is based on 6550 observations.

FIGURE 5. The dynamics of the model.

relatively low. Since the market is dominated by fundamentalists, the price fluctuates around its fundamental value $p^* = 10$ and the market's price volatility is moderate. The impact of technical analysis suddenly starts to increase and prices slowly diverge from the fundamental value. Since it becomes profitable to

https://doi.org/10.1017/S1365100519000774 Published online by Cambridge University Press



Note. The panels show, from top to bottom, the evolution of the price, the corresponding returns, and the weight of chartists between periods 2500 and 3700 of the simulation run depicted in Figure 5, respectively.

FIGURE 6. Functioning of the model.

rely on the technical forecasting rule, more and more agents choose to be chartists and their weight increases further. This causes the price depreciation to continue and volatility goes up. Around period $t = 2900$, the weight of chartists has increased to such an extent that the fundamental steady state becomes unstable.

https://doi.org/10.1017/S1365100519000774 Published online by Cambridge University Press

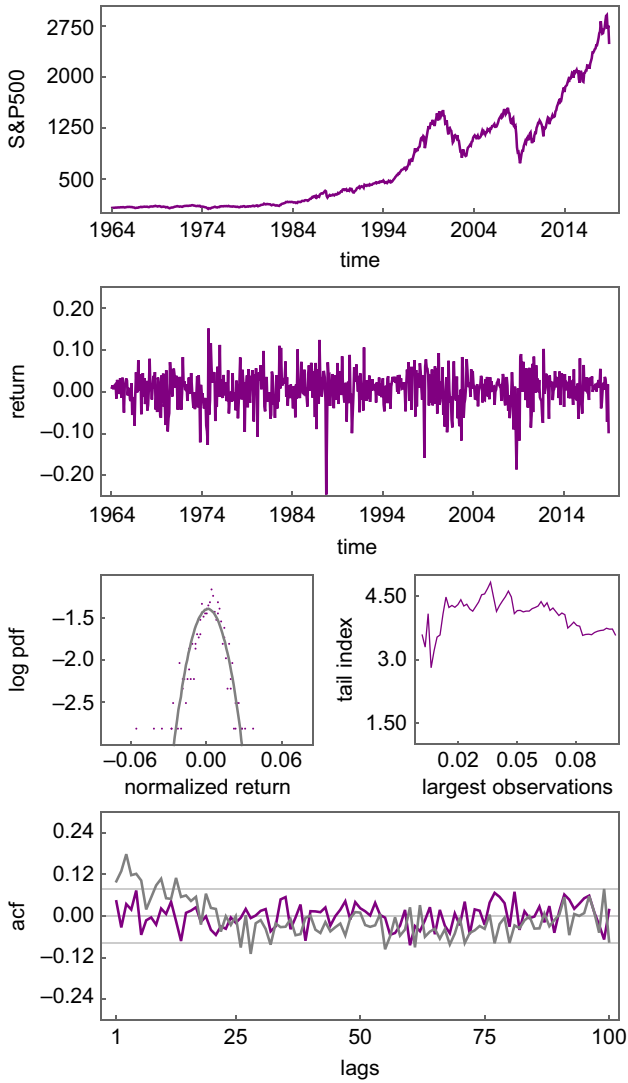
Recall from our deterministic analysis that the fundamental steady state is locally stable if and only if $0.5g + 0.5v < (r + 1)$. Given the estimated parameters $g = 1.001$, $v = 0.989$, and $r = 0.0002$, this condition is obviously satisfied. Out of equilibrium, however, the stability condition can be expressed as $W^C_{t-1}g + (1 - W^C_{t-1})v < (r + 1)$ from which it follows that our system diverges from $p^* = 10$ if $W^C_{t-1} \geq 0.93$.[19] The gray line depicted in the bottom panel of Figure 6 represents this relation. Thus, as soon as the weight of chartists exceeds this critical value, the price disconnects from its fundamental value. In fact, this is exactly what we observe. Between observations 2900 and 3050, the market share of chartists fluctuates around the threshold and there are even longer phases in which their weight is clearly larger than 0.93. As can be seen, asset prices crash during this period and mispricing increases further. However, agents' expectations are also affected by random shocks due to which our system may jump between stable and unstable phases. In particular, the market re-enters the region for which the fundamental steady state is attracting around period $t = 3050$. As mispricing decreases, the fundamental forecasting rule is now more attractive and an increasing number of agents switch to fundamental analysis. This explains why the downward trend comes to a halt and reverses direction. Obviously, prices revert toward the fundamental value and volatility decreases again.

As the price approaches its fundamental value, the profitability of the fundamental expectation rule decreases and the story repeats itself. The market share of chartists starts to recover and prices continue to rise. Since chartists make higher profits, their market share increases further and a bubble emerges. During this process, the fundamental steady state becomes unstable again. Note, however, that the duration and amplitude of bubbles and crashes varies considerably. The destabilizing behavior of chartists also has different effects and extreme price changes may occur. In period $t = 3265$, for instance, the price increases by 8.4%. Such an extreme return occurs if the market impact of chartists is high and if they receive a strong trading signal (either because of the deterministic part of their expectation rules or because of the correlated random shocks reflecting the heterogeneity of their expectations). All in all, the dynamics is driven by the interplay between nonlinear endogenous forces and random shocks affecting agents' expectations.

4.4. Robustness Check

In this section, we want to demonstrate that our results are robust with respect to other time series. For this purpose, we use a time series of the monthly S&P500 between 1964 and 2018, containing 660 observations, and reestimate our model. The dynamics of the corresponding time series is shown in Figure 7. Of course, the design is identical to that of Figure 3. To quantify the statistical properties, we compute the standard deviation of returns V, the Hill tail index $\alpha_{5.0}$, the autocorrelation coefficients of raw returns $ac\ r_i$ for lags $i \in \{1, 2\}$, and the autocorrelation coefficients of absolute returns $ac\ |r_i|$ for lags $i \in \{2, 4, 6, 9, 12, 25\}$. While estimates of these statistics are shown in the first lines of Table 3, we report again

https://doi.org/10.1017/S1365100519000774 Published online by Cambridge University Press



Note. The panels show, from top to bottom, the evolution of the S&P500 between 1964 and 2018, the corresponding returns, the log probability density functions of normalized returns (purple) and standard normally distributed returns (gray), the Hill tail index estimator as a function of the largest returns and the autocorrelation functions of raw returns (purple) and absolute returns (gray), respectively.

FIGURE 7. The dynamics of the monthly S&P500.

the lower and upper boundaries of the 95% confidence intervals of the moments' bootstrapped frequency distributions in the second and third lines. Note that our bootstrapping approach remains the same except that we subdivide the time series for the block bootstrap into 55 blocks with 12 monthly observations each.

https://doi.org/10.1017/S1365100519000774 Published online by Cambridge University Press

TABLE 3. Moments of the monthly S&P500

	V	$\alpha_{5.0}$	$ac\ r_1$	$ac\ r_2$	$ac\ \lvert r_2\rvert$
Measured	4.265	4.159	0.042	−0.033	0.129
Lower bound	3.780	3.547	−0.056	−0.120	0.049
Upper bound	4.737	6.543	0.144	0.055	0.217

	$ac\ \lvert r_4\rvert$	$ac\ \lvert r_6\rvert$	$ac\ \lvert r_9\rvert$	$ac\ \lvert r_{12}\rvert$	$ac\ \lvert r_{25}\rvert$
Measured	0.118	0.102	0.088	0.050	0.000
Lower bound	0.034	0.025	−0.004	−0.019	−0.068
Upper bound	0.216	0.189	0.201	0.122	0.065

Note: The first lines contain estimates of the returns' standard deviation V, the Hill tail index $\alpha_{5.0}$, the autocorrelation coefficients of raw returns $ac\ r_i$ for lags 1 and 2, and the autocorrelation coefficients of absolute returns $ac\ |r_i|$ for lags $i \in \{2, 4, 6, 9, 12, 25\}$. The second and third lines show the lower and upper boundaries of the 95% confidence intervals around the summary statistics that are reported in the first lines. Estimates are based on a time series ranging from January 1964 to December 2018 that contains 660 monthly observations.

To reestimate our model, we employ again the method of simulated moments and search for the parameter setting that maximizes the JMCR score. Since we want to be consistent with our estimation for daily data, we set $p^* = 10$, $a\sigma^2 = 1$, $N = 300$, and $\rho^F = \rho^F$. However, the interest rate is adjusted to $r = \frac{0.05}{12} = 0.004167$, implying that $\bar{y} = 0.04167$. The maximization of the JMCR score yields a value of 28.6% and the following parameter values:

$$g = 1.012,\ v = 0.978,\ \sigma^C = 0.0813,\ \sigma^F = 0.0343,$$
$$\rho^C = \rho^F = 0.78,\ \beta = 63 \text{ and } \mu = 0.94.$$

As to be expected, the two belief parameters g and v become more extreme.[20] Moreover, σ^C remains larger than σ^F and the correlation parameters ρ^C and ρ^F do not change. Finally, parameters β and μ decrease. Of course, a lower memory parameter can easily be explained since time now refers to months and not days. As a result, volatility clustering is less pronounced if we simulate the model for monthly data.

Table 4 also shows the fractions of the individuals moments' matching and makes obvious that our model matches all 10 moments quite well. Note that the average moment matching score is given by 85.9%. To visualize this performance, we depict a representative simulation run in Figure 8. As can be seen, the simulated dynamics are very similar to those depicted in Figure 7. Overall, our model is thus able to explain the daily and monthly behavior of the S&P500.

https://doi.org/10.1017/S1365100519000774 Published online by Cambridge University Press

TABLE 4. Performance of the model

	V	$\alpha_{5.0}$	$ac\ r_1$	$ac\ r_2$	$ac\ \lvert r_3\rvert$
JMCR	0.822	0.790	0.932	0.876	0.936
0.286	$ac\ \lvert r_6\rvert$	$ac\ \lvert r_{12}\rvert$	$ac\ \lvert r_{25}\rvert$	$ac\ \lvert r_{50}\rvert$	$ac\ \lvert r_{100}\rvert$
	0.862	0.836	0.912	0.836	0.788

Note: The table shows the joint moment coverage ratio (JMCR) and the fractions of the individual moments' matching. Estimations are based on 500 simulation runs with 660 observations each. Parameters are $r = 0.004167$, $F = 10$, $\bar{y} = 0.04167$, $a\sigma^2 = 1$, $N = 300$, $g = 1.012$, $v = 0.978$, $\sigma^F = 0.0343$, $\sigma^C = 0.0813$, $\rho^C = \rho^F = 0.78$, $\beta = 63$, and $\mu = 0.94$.

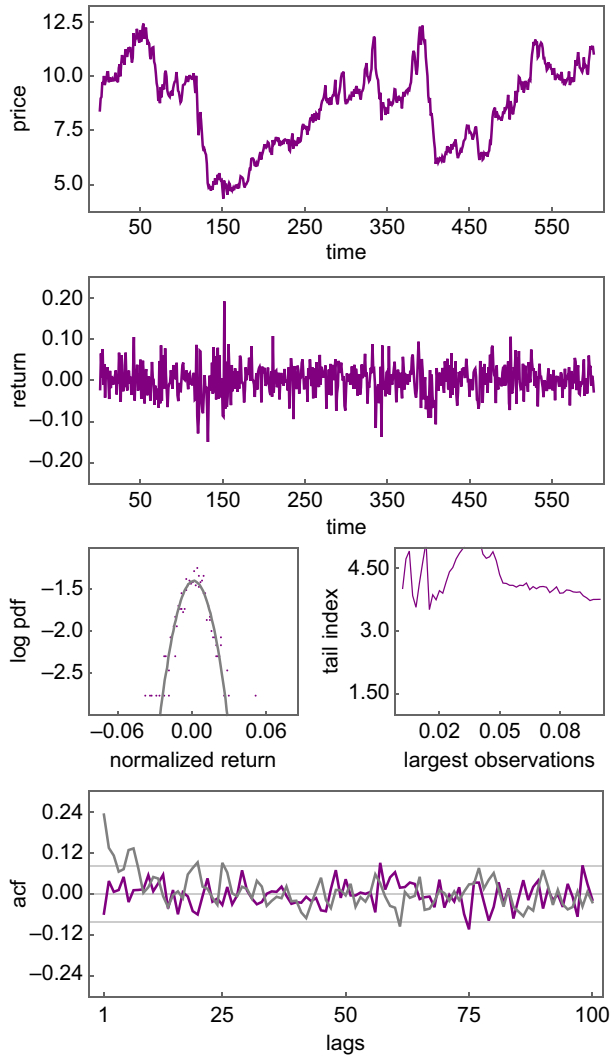
5. CONCLUSIONS

In this paper, we generalize the seminal model by Brock and Hommes (1998) by considering that all agents follow their own individual technical and fundamental expectation rules. While their forecasts may be correlated to some degree, all agents have different expectations about future asset prices. As a result, the agents' demands, their rules' fitness and, consequently, their discrete choice probabilities differ. In this sense, we provide an agent-based setup for the model by Brock and Hommes (1998). Since heterogeneity is a key characteristic of financial markets, such a model extension seems to be worthwhile.

Moreover, we demonstrate that our model version can explain the stylized facts of stock markets. By estimating our model using the method of simulated moments, we find that our approach matches the daily behavior of the S&P500 quite well. In particular, our analysis reveals that we match in 33% of the simulation runs all 10 summary statistics that are used to quantify the main stylized facts of stock markets. For monthly data, our model generates similar scores. Crucial for the striking performance of our model is the assumption that agents have heterogeneous expectations, that is, the model's performance would weaken dramatically if agents' choices were restricted to a representative technical and a representative fundamental expectation rule. By providing empirical support for the Brock and Hommes (1998) model on the basis of daily and monthly data, we also complement the studies by Boswijk et al. (2007) and Hommes and 't Veld (2017), which rely on yearly and quarterly data, respectively.

Finally, our approach also offers a novel explanation for the intricate behavior of stock markets. Our analytical results indicate that the model's fundamental steady state is locally stable for the estimated parameter setting. Out of equilibrium, however, the market impact of technical expectation rules may temporarily increase and render the fundamental steady state unstable. Suppose, for instance, that the asset price increases above its fundamental value. In such a situation, technical expectation rules tend to be more profitable than fundamental expectation rules. As the market impact of technical expectation rules grows, the

https://doi.org/10.1017/S1365100519000774 Published online by Cambridge University Press



Note. The panels show, from top to bottom, the evolution of the price, the returns, the log probability density functions of normalized returns (purple) and standard normally distributed returns (gray), the Hill tail index estimator as a function of the largest returns and the autocorrelation functions of raw returns (purple) and absolute returns (gray), respectively. The simulation run is based on 660 observations.

FIGURE 8. The dynamics of the model.

momentum of the price increase is likely to continue and may create a bubble. Such a development is usually accompanied by a period of higher volatility and the occasional occurrence of larger price changes. Eventually, however, the bubble comes to a halt and reverses direction. Now fundamental expectation rules

https://doi.org/10.1017/S1365100519000774 Published online by Cambridge University Press

outperform technical expectation rules, and the market once again enters a more stable phase. In particular, asset prices are driven closer toward the fundamental value, price variability tends to shrink, and extreme price changes are observed less frequently. Thus, the dynamics switch back and forth between stable and unstable phases. Due to the large heterogeneity of the expectation rules applied, asset price changes are serially uncorrelated. Of course, agents' disagreement about the future direction of the market keeps them trading and is thus responsible for the excessive price volatility.

Our approach may be extended in various directions. First of all, we assume that the correlation between agents' expectation rules is constant. One interesting extension of our model may be to consider a time-varying correlation. Keynes (1936) already argued that people tend to herd more strongly in periods with heightened uncertainty. Hence, the correlation between agents' expectation rules may, for instance, be conditioned on market uncertainty. Moreover, the rule selection behavior of an agent is assumed to depend on the experience he has with his own rules. Alternatively, one could consider agents talking to each other and basing their rule selection, that is, the choice between extrapolative and regressive expectation rules, on the average profitability of these rules within their peer group. Agents' rule selection may furthermore depend on herding effects or on market conditions such as observed mispricing. From an econometric perspective, it may also be worthwhile estimating our model for other financial markets. One advantage of our estimation strategy is that it does not rely on any assumption about a market's fundamental value, which is, obviously, difficult to quantify. Nevertheless, one may follow Shiller (2015) approach on how to compute the fundamental value of the S&P500. In doing so, one may add a distortion measure to the list of moments and seek to match the S&P500's boom-and-bust dynamics.

However, we would like to conclude our paper by pointing out once again that heterogeneity matters in financial markets. By allowing for more heterogeneity, we show that the seminal asset-pricing model by Brock and Hommes (1998) becomes not only more realistic but also has the potential to explain the daily and monthly behavior of stock markets.

NOTES

1. Similarly, Diks and van der Weide (2003, 2005) generalize the notion of LTL and develop a simple continuous beliefs system to model the co-evolution of prices and the beliefs distribution explicitly.

2. Gaunersdorfer (2000) studies the case in which agents' beliefs about conditional variances are time-varying and observes, at least in the case of an IID dividend process, similar dynamics as in the original model by Brock and Hommes (1998).

3. Brock (1997) gives a justification for the simplifying case $z^s = 0$ by introducing risk-adjusted dividends.

4. Questionnaire studies by Menkhoff and Taylor (2007) or Jongen et al. (2012) as well as laboratory experiments by Hommes (2011) strongly support this assumption.

5. To avoid variability of the noise-to-price-ratio, random shocks are normalized with most recent prices (see Franke (2010)).

https://doi.org/10.1017/S1365100519000774 Published online by Cambridge University Press

6. Note that $Var\left(\frac{1}{N^j}\sum_{i=1}^{N^j}\epsilon_t^{j,i}\right) = \rho^j + \frac{1-\rho^j}{N^j} \to \rho^j$ as $N^j \to \infty$, where $j = C, F$. This implies that the central limit theorem does not hold if $\rho^j \neq 0$. Moreover, for a sufficiently large number of agents, a further increase in N^j has almost no impact on $Var\left(\frac{1}{N^j}\sum_{i=1}^{N^j}\epsilon_t^{j,i}\right)$ which is why we will not estimate parameter N $(= N^C + N^F)$. For $\rho^j = 0$ and $N \to \infty$, the trading rules' random digressions wash out and the dynamics converge toward the model's deterministic skeleton.

7. Gaunersdorfer et al. (2008) provide an analysis of this model with risk-adjusted realized profits as the fitness measure.

8. Note that realized excess returns depend on stochastic dividends, that is, $y_t = \bar{y} + \epsilon_t$, where ϵ_t is IID. However, we follow the main scenario of Brock and Hommes (1998) and focus on the deterministic case by setting $\epsilon_t = 0$.

9. In Brock and Hommes (1998), the fundamental expectation rule is costly. They substantiate this assumption by arguing that agents face constant per period information costs for obtaining the fundamental value. In our setup, both predictors rely on the fundamental value, which is why we abstain from (differences in) information costs.

10. Note that several versions of the Brock and Hommes (1998) model already have been investigated analytically. However, our model differs in several dimensions from these setups. For instance, we model forecasts about future prices as in Boswijk et al. (2007), we include the memory parameter μ, and we abstain from information costs. Due to the one-to-one correspondence between the deterministic and the stochastic model, our analytical results allow a clear interpretation of our estimated parameters.

11. Recall that $W_t^C = \frac{N_t^C}{N}$ and $N_t^C = \sum_{i=1}^{N} I_t^i$. Since I_t^i is binomial distributed, we have, for $N \to \infty$, $E[W_t^C] = \pi_t^C = \frac{\exp[\beta U_t^C]}{\exp[\beta U_t^C]+\exp[\beta U_t^F]}$ and $Var[W_t^C] = \frac{\pi_t^C(1-\pi_t^C)}{N} = 0$. Of course, the same arguments apply for the fraction of fundamentalists.

12. Since $W_t^C + W_t^F = 1$ and $m_t = W_t^F - W_t^C$, we have $W_t^C = \frac{1-m_t}{2}$ and $W_t^F = \frac{1+m_t}{2}$. Moreover, $U_t^F - U_t^C$ can be rewritten as $\frac{2\,\mathrm{arctanh}[m_t]}{\beta}$.

13. Of course, other model parameters may also influence the stability of our deterministic model dynamics. For instance, decreasing values of v and increasing values of r may stabilize the system. Note that the intensity of choice has no effect on the stability of our steady states. The reason for this is as follows. Since we abstain from (differences in) information costs, the two predictors yield identical profits at the steady state. Thus, β has no influence at the steady state as there are no profit differences. Out of equilibrium, increasing values of β do reduce the price deviation. This is intuitively clear, since higher values for the intensity of choice make agents more sensitive in selecting the most profitable forecast. As more agents then opt for fundamental analysis, the price deviation decreases.

14. Note that the eigenvalues of (31) can now be computed and are given by $\lambda_1 = -0.041$, $\lambda_2 = 0.988 + 0.289i$, and $\lambda_3 = 0.988 - 0.289i$. Since $|\lambda_{2/3}| = 1.06$, the complex eigenvalues have just crossed the unit circle and Figure 2 illustrates a situation shortly after the Neimark–Sacker bifurcation.

15. Further simulations reveal that our results are robust with respect to other values of the interest rate.

16. Let us put this value into a quantitative perspective. By considering the events that the sample moments from the true data generating process (DGP) fall into their confidence intervals and assuming that these events are all independent from each other, we would obtain a JMCR score of $0.95^{10} = 0.5987$ for the true DGP. Of course, not all of these events are independent from each other. Assuming that only five of them, for instance, are independent would yield a value of 0.774. Franke and Westerhoff (2012), for instance, consider 9 moments and obtain a JMCR score of 0.266.

17. Note that the empirical intervals of the raw returns' autocorrelations are centered around $ac\ r_1 = -0.059$ and $ac\ r_2 = -0.041$. Since a stock market's return dynamics usually shows no sign of predictability, we adjusted the empirical intervals of the two summary statistics by setting their lower and upper boundaries to -0.04 and 0.04, ensuring that we have bands that are symmetric around zero and almost equally sized as those computed from the bootstrapped distributions.

18. We would like to stress two important observations. First, chartists indeed extrapolate past deviations and fundamentalists indeed drive prices back toward the fundamental value. Second, the

https://doi.org/10.1017/S1365100519000774 Published online by Cambridge University Press

JMCR score decreases significantly when we deviate from $\rho^C = \rho^F = 0.78$. This implies that our estimation results are in line with the empirical evidence reported in the introduction: while agents' forecasts are heterogeneous, their expectations are also correlated to some degree. To emphasize the importance of the heterogeneity, we also estimated a model version where $\rho^C = \rho^F = 1$ and obtain a JMCR score of 28.8%. Thus, we gain 12.5% in explanatory power when we assume heterogeneity among agents. However, the model version where $\rho^C = \rho^F = 1$ is still agent-based since each agent decides individually whether to follow the technical or the fundamental forecasting rule.

19. Note that Boswijk et al. (2007) and Hommes and 't Veld (2017) perform a similar analysis by using the concept of the *average market sentiment.*

20. Boswijk et al. (2007) and Hommes and 't Veld (2017) estimate the same belief parameters using nonlinear least squares on the basis of yearly and quarterly data of the S&P500, respectively. For instance, Boswijk et al. (2007) report that $g \approx 1.1$ and $v \approx 0.8$, implying that chartists (fundamentalists) believe that the deviation from the fundamental value will increase (decrease) by 10 (20) percent over the next year. These numbers are about 10 times larger than our estimates for monthly data – which sounds quite reasonable. For quarterly data, Hommes and 't Veld (2017) find values that lie in between. Taking also our estimates for daily data into account, we can conclude that parameters g and v become more extreme when the forecasting horizon is longer.

REFERENCES

Anufriev, M. and C. Hommes (2012) Evolutionary selection of individual expectations and aggregate outcomes in asset pricing experiments. *American Economic Journal: Microeconomics* 4, 35–64.

Anufriev, M. and J. Tuinstra (2013) The impact of short-selling constraints on financial market stability in a heterogeneous agents model. *Journal of Economic Dynamics and Control* 37, 1523–1543.

Boswijk, H. P., C. Hommes and S. Manzan (2007) Behavioral heterogeneity in stock prices. *Journal of Economic Dynamics and Control* 31, 1938–1970.

Brock, W. (1997) Asset price behavior in complex environments. In: W. Brian Arthur, S. N. Durlauf and D. A. Lane (eds.), *The Economy as an Evolving Complex System II*, pp. 385–423. Reading: Addison-Wesley.

Brock, W. and C. Hommes (1997) A rational route to randomness. *Econometrica* 65, 1059–1095.

Brock, W. and C. Hommes (1998) Heterogeneous beliefs and routes to chaos in a simple asset pricing model. *Journal of Economic Dynamics Control* 22, 1235–1274.

Brock, W., C. Hommes and F. Wagener (2005) Evolutionary dynamics in markets with many trader types. *Journal of Mathematical Economics* 41, 7–42.

Brock, W., C. Hommes and F. Wagener (2009) More hedging instruments may destabilize markets. *Journal of Economic Dynamics and Control* 33, 1912–1928.

Chiarella, C., R. Dieci and X.-Z. He (2009) Heterogeneity, market mechanisms, and asset price dynamics. In: T. Hens and K. R. Schenk-Hoppé (eds.), *Handbook of Financial Markets: Dynamics and Evolution*, pp. 277–344. Amsterdam: North-Holland.

Cont, R. (2001) Empirical properties of asset returns: Stylized facts and statistical issues. *Quantitative Finance* 1, 223–236.

Cont, R. and J.-P. Bouchaud (2000) Herd behaviour and aggregate fluctuations in financial markets. *Macroeconomic Dynamics* 4, 170–196.

Day, R. H. and W. Huang (1990) Bulls, bears and market sheep. *Journal of Economic Behavior and Organization* 14, 299–329.

De Grauwe, P. and M. Grimaldi (2006) Exchange rate puzzles: A tale of switching attractors. *European Economic Review* 50, 1–33.

Diks, C. and R. van der Weide (2003) Heterogeneity as a natural source of randomness. Tinbergen Institute Discussion Paper No. 2003-073/1. Available at SSRN: https://ssrn.com/abstract=452381.

Diks, C. and R. van der Weide (2005) Herding, a-synchronous updating and heterogeneity in memory in a CBS. *Journal of Economic Dynamics and Control* 29, 741–763.

https://doi.org/10.1017/S1365100519000774 Published online by Cambridge University Press

Franke, R. (2009) Applying the method of simulated moments to estimate a small agent-based asset pricing model. *Journal of Empirical Finance* 16, 804–815.
Franke, R. (2010) On the specification of noise in two agent-based asset pricing models. *Journal of Economic Dynamics Control* 34, 1140–1152.
Franke, R. and F. Westerhoff (2012) Structural stochastic volatility in asset pricing dynamics: Estimation and model contest. *Journal of Economic Dynamics and Control* 36, 1193–1211.
Franke, R. and F. Westerhoff (2016) Why a simple herding model may generate the stylized facts of daily returns: Explanation and estimation. *Journal of Economic Interaction and Coordination* 11, 1–34.
Gaunersdorfer, A. (2000) Endogenous fluctuations in a simple asset pricing model with heterogeneous agents. *Journal of Economic Dynamics and Control* 24, 799–831.
Gaunersdorfer, A., C. Hommes and F. Wagener (2008) Bifurcation routes to volatility clustering under evolutionary learning. *Journal of Economic Behavior and Organization* 67, 27–47.
Gilli, M. and P. Winker (2003) A global optimization heuristic for estimating agent based models. *Computational Statistics and Data Analysis* 42, 299–312.
Graham, B. and D. L. Dodd (1951) *Security Analysis*. New York: McGraw-Hill.
Hill, B. M. (1975) A simple general approach to inference about the tail of a distribution. *Annals of Statistics* 3, 1163–1174.
Hommes, C. (2011) The heterogeneous expectations hypothesis: Some evidence from the lab. *Journal of Economic Dynamics and Control* 35, 1–24.
Hommes, C. (2013) *Behavioral Rationality and Heterogeneous Expectations in Complex Economic Systems*. Cambridge: Cambridge University Press.
Hommes, C. and D. in 't Veld (2017) Booms, busts and behavioural heterogeneity in stock prices. *Journal of Economic Dynamics and Control* 80, 101–124.
Hommes, C., J. Sonnemans, J. Tuinstra and H. van de Velden (2005) Coordination of expectations in asset pricing experiments. *Review of Financial Studies* 18, 955–980.
Hommes, C., J. Sonnemans, J. Tuinstra and H. van de Velden (2008) Expectations and bubbles in asset pricing experiments. *Journal of Economic Behavior and Organization* 67, 116–133.
Ito, T. (1990) Foreign exchange rate expectations: Micro survey data. *The American Economic Review* 80, 434–449.
Jongen, R., W. F.C. Verschoor, C. C. P. Wolff and R. C. J. Zwinkels (2012) Explaining dispersion in foreign exchange expectations: A heterogeneous agent approach. *Journal of Economic Dynamics and Control* 36, 719–735.
Keynes, J. M. (1936) *The General Theory of Employment, Interest, and Money*. New York: Harcourt, Brace and Company.
Kirman, A. (1993) Ants, rationality, and recruitment. *Quarterly Journal of Economics* 108, 137–156.
LeBaron, B. (2006) Agent-based computational finance. In: L. Tesfatsion and K. L. Judd (eds.), *Handbook of Computational Economics: Agent-Based Computational Economics*, pp. 1187–1233. Amsterdam: North-Holland.
LeBaron, B., W. Brian Arthur and R. Palmer (1999) Time series properties of an artificial stock market. *Journal of Economic Dynamics and Control* 23, 1487–1516.
Lux, T. (1995) Herd behaviour, bubbles and crashes. *The Economic Journal* 105, 881–896.
Lux, T. (2009) Stochastic behavioural asset-pricing models and the stylized facts. In: T. Hens and K. R. Schenk-Hoppé (eds.), *Handbook of Financial Markets: Dynamics and Evolution*, pp. 161–216. Amsterdam: North-Holland.
Lux, T. and M. Ausloos (2002) Market fluctuations I: Scaling, multiscaling, and their possible origins. In: A. Bunde, J. Kropp and H. J. Schellnhuber (eds.), *Science of Disaster: Climate Disruptions, Heart Attacks, and Market Crashes*, pp. 373–410. Berlin: Springer.
MacDonald, R. and I. W. Marsh (1996) Currency forecasters are heterogeneous: Confirmation and consequences. *Journal of International Money and Finance* 5, 665–685.
Mantegna, R. N. and E. Stanley (2000) *An Introduction to Econophysics*. Cambridge: Cambridge University Press.

https://doi.org/10.1017/S1365100519000774 Published online by Cambridge University Press

Manski, C. F. and D. McFadden (1981) *Structural Analysis of Discrete Data with Econometric Applications*. Cambridge: MIT Press.
Menkhoff, L. and M. P. Taylor (2007) The obstinate passion of foreign exchange professionals: technical analysis. *Journal of Economic Literature* 45, 936–972.
Menkhoff, L., R. R. Rebitzky and M. Schröder (2009) Heterogeneity in exchange rate expectations: evidence on the chartist-fundamentalist approach. *Journal of Economic Behavior and Organization* 70, 241–252.
Murphy, J. J. (1999) *Technical Analysis of Financial Markets*. New York: New York Institute of Finance.
Schmitt, N. and F. Westerhoff (2017) Heterogeneity, spontaneous coordination and extreme events within large-scale and small-scale agent-based financial market models. *Journal of Evolutionary Economics* 5, 1041–1070.
Shiller, R. J. (2015) *Irrational Exuberance*. Princeton: Princeton University Press.
Ter Ellen, S., W. F. C. Verschoor and R. C. J. Zwinkels (2013) Dynamic expectation formation in the foreign exchange market. *Journal of International Money and Finance* 37, 75–97.
Trueman, B. (1994) Analysts forecasts and herding behavior. *Review of Financial Studies* 7, 97–124.
Welch, I. (2000) Herding among security analysts. *Journal of Financial Economics* 58, 369–396.
Westerhoff, F. and R. Dieci (2006) The effectiveness of Keynes–Tobin transaction taxes when heterogeneous agents can trade in different markets: a behavioral finance approach. *Journal of Economic Dynamics Control* 30, 293–322.
Westerhoff, F. and R. Franke (2012) Converse trading strategies, intrinsic noise and the stylized facts of financial markets. *Quantitative Finance* 12, 425–436.
Winker, P., M. Gilli and V. Jeleskovic (2007) An objective function for simulation based inference on exchange rate data. *Journal of Economic Interaction and Coordination* 2, 125–145.

https://doi.org/10.1017/S1365100519000774 Published online by Cambridge University Press